# Coherent Structures of Transitional Boundary Layers in a Linear Compressor Cascade

Vejapong Juttijudata[1,*] and Sirod Sirisup[2]

[1] Department of Aerospace Engineering, Faculty of Engineering, Kasetsart University, Bangkok, Thailand 10900

[2] Large-Scale Simulation Research Laboratory, National Electronics and Computer Technology Center, Pathumthani, Thailand 12120

* Corresponding Author: Tel: 02 942 8555 Ext. 1708, Fax: 02 579 8570,

E-mail: vejapong.j@ku.ac.th

***Abstract***

The objective of this study is to objectively identify coherent structures of transitional boundary layers in a linear compressor cascade. The database for the analysis is from Direct Numerical Simulation (DNS) of flow through the linear compressor cascade with incoming free-stream turbulence performed by Zaki *et al* [*ASME Turbo Expo, 2006, GT2006-90885*]. On the pressure side, the boundary layer undergoes a bypass transition. On the contrary, on the suction side, the boundary layer is stabilized and remains laminar in a favourable pressure gradient zone. Farther downstream, the laminar boundary layer experiences a strong adverse pressure gradient causing it to separate. The separation induces transition to turbulence, which, in turn, is followed by turbulent reattachment of the detached boundary layer. In order to objectively identify coherent structures in the boundary layers on pressure and suction side of the compressor blade, the Proper Orthogonal Decomposition (POD) is used in the analysis. POD extracts the most-energetic coherent structures from the boundary layers and their energy contents. Coherent structures from POD in the boundary layers of pressure and suction sides are resemble to structures detected by other visualisation methods: elongated streamwise streak or perturbation jets whose averages are known as Klebanoff modes, and travelling-wave structures which may be associated with transition and turbulence production mechanisms. Future work includes the study of the localised POD of two sub-domains namely the boundary layer of pressure and suction side sub-domains in order to obtain more compact description of the transition processes in the compressor cascade.

***Keywords****:* coherent structures, bypass transition, separation-induced transition, Proper Orthogonal Decomposition (POD), compressor cascade

## 1. Introduction

Laminar-turbulent transition phenomena play an important role and have a great impact on the design of modern gas turbine engines. Despite that the flow in gas turbines is highly turbulent and unsteady, the boundary layers on the surfaces may be either laminar or turbulent depending on operating conditions [1]. In order to predict losses and heat transfer on various components in the engine, the understanding of

transition processes on the boundary layers is very crucial. Transition processes in a compressor passage have only been extensively studied in the last decade. Numerical studies by means of direct numerical simulations (DNS) only appeared recently in [2,3]. One of the main conclusions of these studies is transition phenomena and processes in a compressor passage are quite complex and required further analysis in order to obtain a better understanding and insight.

In the light of coherent structures, complex transitional boundary layers may be decomposed into coherent motion or coherent structures, and incoherent motion [4] allowing the backbone of transition processes to surface up. Many techniques have been used to identify coherent structures in transitional and turbulent flows. The proper orthogonal decomposition (POD) is one of the most popular and successful techniques to objectively extract the most energetic structures defined as coherent structures in the flow [4]. The POD and POD-based reduced-order models shed light on turbulence production mechanisms in many flows (see review in [4]) as well as transition process of natural transition on a flat-plate boundary layer [5,6]. The result in [5,6] underlines that in the light of the coherent structures approach, a compact description of transition process in the transitional boundary layer can be obtained.

The objective of this study is to identify coherent structures of transitional boundary layers in a linear compressor cascade by means of the POD. The result of this work will be the basis to study the transition processes and mechanisms in the on-going project.

## 2. DNS of transition in a compressor passage

In this study, the database for the analysis is from DNS of flow through the linear V103 compressor cascade [7] with incoming free-stream turbulence performed by [2]. The computational domain and boundary conditions are shown in Fig. 1. The pitch of the blade is set to 0.59 $L$, where $L$ is the axial chord of the compressor blade with spanwise period of 0.2 $L$. At inlet, grid turbulence is superimposed on the mean field. The turbulent intensity is 3.2% at the inlet plane and dropping to 2.5% at the leading edge of the blade. The distortion creates some anisotropy of the free-stream turbulence but the effect is small. The simulation is based on a local volume flux formulation in curvilinear coordinates on a staggered grid [8]. Adams-Bashfort, implicit Euler and Crank-Nicolson time-integrator are used to treat convective, pressure and diffusion terms, respectively. Grid in the simulation is also shown in Fig. 1 comprising of 1025 x 641 x 129 grid points in tangential to the flow, cross-stream, and spanwise directions, respectively. The Reynolds number of the flow based on freestream velocity $U_0$ and axial chord $L$ is $Re$ = 138,500.

Pressure and skin-friction coefficients of pressure and suction sides of the compressor blade are shown in Fig. 2. On the pressure side (Fig. 2a), the boundary layer under high free-stream turbulence is attached and undergoes a bypass transition starting from $x/L$ = 0.22 and completed at $x/L$ = 0.46 without separation despite of the existing of a long adverse-pressure gradient zone. In bypass transition,

low-frequency disturbances in the free-stream penetrate into the boundary layer and create elongated streamwise streaks or perturbation jets and their time averages are known as Klebanoff modes or distortions shown in the top blade in Fig. 3. These perturbation jets are lifted up into the upper part of the boundary layer and triggered to instability and transition by high-frequency disturbances in the free-stream. The effects of adverse and favourable pressure gradients (APG and FPG) are to promote and suppressed Klebanoff mode instability and transition, respectively, as clearly seen in the bottom blade of Fig. 3.

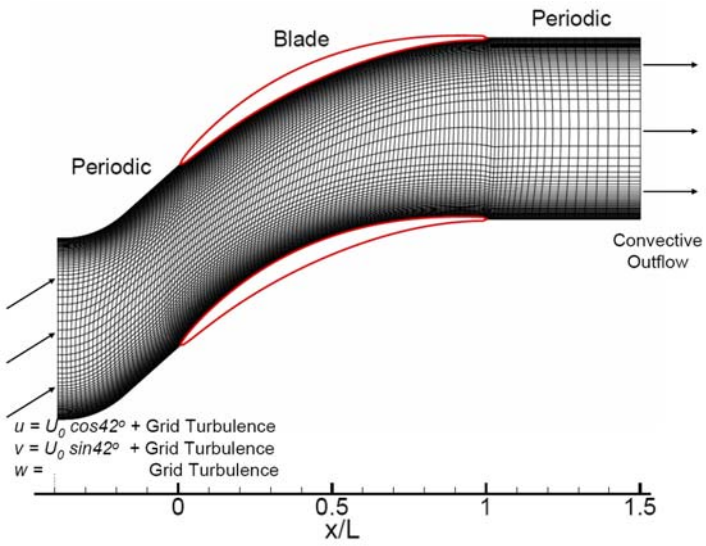


Fig. 1 Computational domain, grid (only the 8th grid lines shown), and boundary conditions.

On the contrary, on the suction side (Fig. 2b), the boundary layer is stabilized and remains laminar in a favourable pressure gradient zone. Farther downstream, the laminar boundary layer experiences a strong adverse pressure gradient causing it to separate at *x/L* = 0.45. Two-dimensional Kelvin-Helmholtz billows appear in the unsteady detached shear layer after the separation point. Kelvin-Helmholtz billows quickly breakdown into three-dimensional disturbances leading to transition to turbulence. Turbulent detached shear layer reattaches the surface of the suction side again at *x/L* = 0.70 forming a separation bubble. Effect of pressure gradients on Klebanoff modes are clearly seen in Fig. 3.

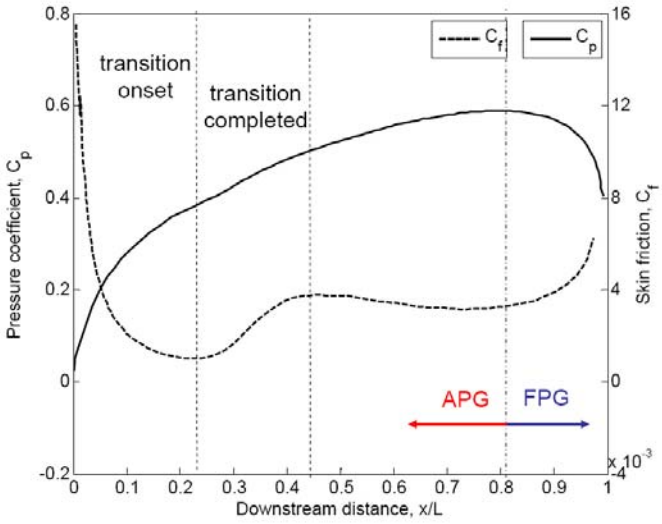


(a)

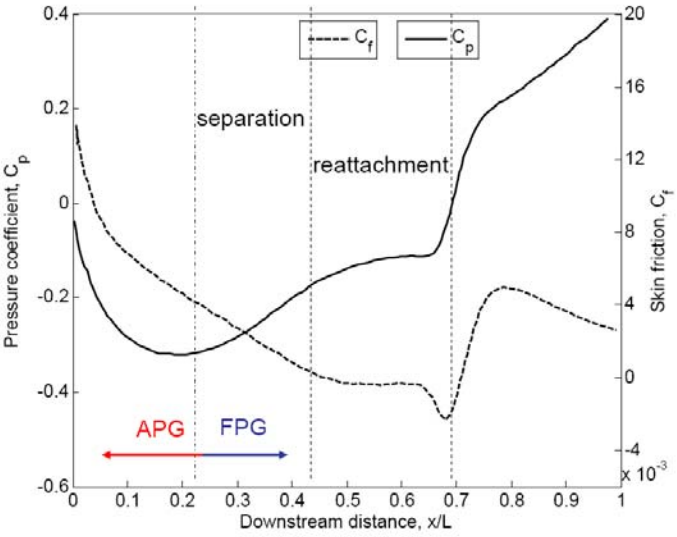


(b)

Fig. 2 Pressure and skin-friction coefficients on the pressure side (a) and suction side (b) of the compressor blade. Important locations are also marked in the figure.

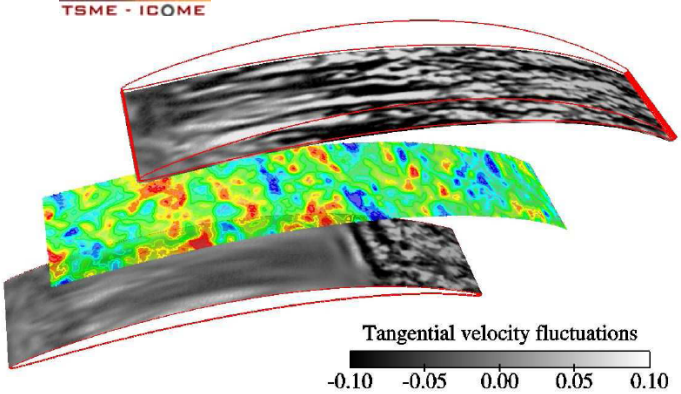


Fig. 3 Contours of tangential velocity perturbation from the mean velocity on the pressure (top) and suction (bottom) sides together with that of free-stream turbulence in the centre-plane of the passage (Taken from [2]).

### 3. Proper orthogonal decomposition (POD)

In order to extract coherent structures from a given ensemble of the given flow fields, the method of "snapshots" [9] is employed. Specifically, let $\boldsymbol{V}(\boldsymbol{x},t)$ be a given flow field and the ensemble $\{\boldsymbol{V}(\boldsymbol{x},t_k)\}_{k=1}^{N}$ be a collection of such flow field at observation time $t_k$ for $k=1,\ldots,N$ i.e. the flow "snapshots". By decomposing the flow field into mean velocity, $\boldsymbol{U}_0$, and velocity fluctuation, $\boldsymbol{u}(\boldsymbol{x},t)$ i.e. $\boldsymbol{V}(\boldsymbol{x},t) = \boldsymbol{U}_0 + \boldsymbol{u}(\boldsymbol{x},t)$, the eigenmode $\Phi_i$ may be defined as

$$\Phi_i = \sum_{k=1}^{N} w_k^i u^k, i = 1,\ldots,N \cdot \qquad (1)$$

Here, $\boldsymbol{u}^k = \boldsymbol{u}(\boldsymbol{x},t_k)$ and $w_k^i$ are the components of the eigenvector $\boldsymbol{W}^i$ derived from the eigenvalue problem

$$CW = \lambda W \qquad (2)$$

where, $\boldsymbol{C}$ is the spatial correlation matrix defined by

$$C_{ij} = \frac{1}{N}\int_{\Omega} u^i \cdot u^j d\Omega \cdot \qquad (3)$$

The eigenvalue corresponding to each eigenvector from Eq. (2) represents the energy content in that eigenvector and eigenmode. Note that the spanwise reflection [9] i.e.

$$\begin{aligned} u(x,y,z,t_i) &= u(x,y,-z,t_i) \\ v(x,y,z,t_i) &= v(x,y,-z,t_i) \cdot \\ w(x,y,z,t_i) &= w(x,y,-z,t_i) \end{aligned} \qquad (4)$$

is imposed in order to increase the size of the ensemble to improve the convergence rate of the POD. Furthermore, the spanwise reflection ensures spanwise reflection in statistical sense in the eigenmodes. Here *x, y, z, u, v* and *w* are position and velocity components in local tangential to the flow, cross-stream, and spanwise directions, respectively.

### 4. Results

The POD is performed in the passage only without domains before and after the passage i.e $0 \le x/L \le 1$. The DNS data at every other grid point are obtained from the time span of 1.1250 $L/U_0$ constituting 400 snapshots in the ensemble. By imposing the spanwise reflection, the number of snapshots in the ensemble is doubled. The data are in a single precision format. The eigenvalue solver used is a double precision LAPACK eigenvalue solver for symmetric matrix.

The normalised eigenvalue i.e. energy content in each mode relative to the total energy content in the flow is shown in Fig. 4. The eigenvalues (energy contents) of the first mode is three times, and the second and third modes are twice more than those of the fourth mode. The eigenvalues decay as the order of the eigenmode increased nevertheless the decaying rate is not as rapid as that found in any of flows. This suggests the flow in this study is relatively complex and required many modes to describe its dynamics accurately. This is not so surprise as this flow actually has three different flow dynamics corresponding to bypass transition in boundary layer on pressure side, separation-

induced transition on suction side as well as the distortion of grid turbulence in the middle of the passage. On top of that, their interactions also contribute to the eigenvalues and eigenmodes in this study. For this study, only the first four modes accounting of 10% of the total energy content of the flow will be first focused as their energy contents in the first three modes are dominated the other modes, and the fourth mode tends to couple with first mode as will be seen later.

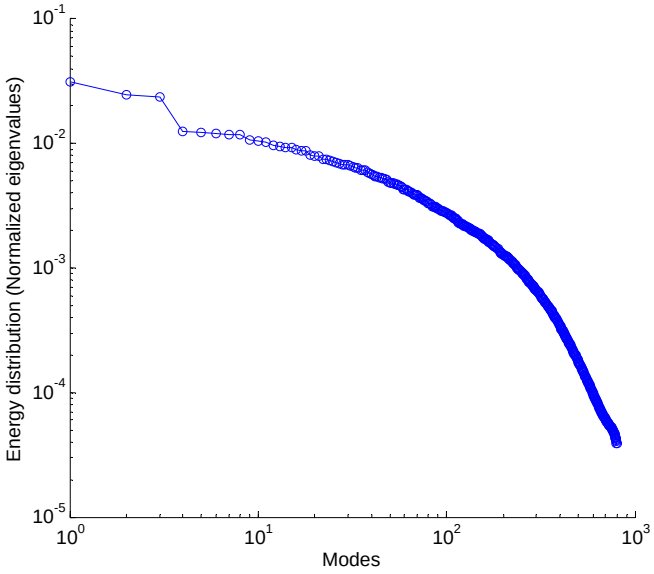


Fig. 4 Energy distribution (normalised eigenvalues) of different POD modes

Figs 5 – 8 show the isosurfaces of tangential components of the first four eigenmodes, respectively. Orange and purple represent negative and positive values, respectively, and the darker orange and blue indicate high negative and positive values, respectively.

The striking feature of the first mode (Fig. 5) is the presence of elongated streamwise streaks, and perturbation jets or Klebanoff modes on both pressure and suction sides similar to that found in flow visualization in [2]. On pressure side (top blade), where boundary layer undergoes bypass transition, Klebanoff modes are the dominated coherent structures as visualised in transition zone. Elongated streamwise streak also contributes to the first mode in fully-turbulent zone. On the suction (suction blade), where boundary layer undergoes separation-induced transition, most energetic structures are corresponding to Klebanoff modes within separation bubble and streamwise streaks in reattachment zone with the highest peak slightly upstream of the reattachment close to the breaking down to three-dimensional disturbances of Kelvin-Helmholtz instability point. High level of tangential component in the separation bubble zone further underlines that adverse pressure gradient intensifies Klebanoff modes [2].

Mode 2 and 3 share pretty similar feature that is alternating values of positive and negative values in the flow direction (Figs 6 and 7). This feature suggests the presence of travelling-wave structures in the flow direction associated with turbulence production mechanism in fully-turbulent flows [10]. On pressure side, peaks positive and negative values lie close in transition zone. Travelling-wave structures in transition zone may suggest transition mechanism. However, further study is required as there is no literature, to authors' best knowledge, has ever reported this. On suction side, these peak values locate slightly downstream of the reattachment point in fully-turbulent zone; these traveling-wave structures here may associate with turbulence production mechanism of reattached turbulent boundary layer rather than transition mechanism or

breaking down into three-dimensional disturbances of Kelvin-Helmholtz instability. Further study is required to further confirm the postulation.

Mode 4 in Fig. 8 shows a mixed feature of elongated streamwise streaks or Klebanoff modes on the pressure side, and traveling-wave structures on the suction side. Klebanoff modes on the pressure side of this mode have a higher wavenumber in spanwise direction or a shorter integral scale compared to those of first mode. For the suction side, the travelling-wave structure of this mode has a longer wavelength than those in mode 2 and 3. Furthermore the peak values occurs almost at the mean reattachment line suggesting that the travelling-wave structure here may associate with some wave disturbances triggering the breaking down into three-dimensional disturbances of Kelvin-Helmholtz instability and convected downstream. Again, this speculation needs further analysis and justification.

To gain some insight of their dynamics and interactions, spectral analysis of the temporal modes i.e. the eigenvector from Eq. (2), shown in Fig. 9, is performed. Clearly mode 1 and 4 closely interact to each other at rather low frequency (0.89 $U_0/h$) while mode 2 and 3 interact to each other at much higher frequency (6.22 $U_0/h$). From energy spectrum in [2], mode 1 and 4 are most likely to associate with Klebanoff modes whereas mode 2 and 3, not as clear as mode 1 and 4, may be associated to turbulence production mechanism or the breaking down of Kelvin-Helmholtz instability. Note that the energy at the dominant frequency of the first mode is lower than those of other modes but the total energy across the frequency domain of the first mode is the largest one.

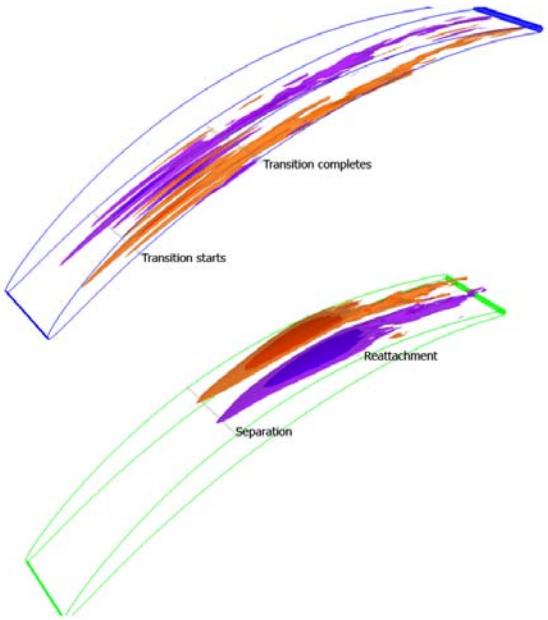


Fig.5 Isosurfaces of tangential component of the eigenmode 1. Orange (purple) and dark orange (purple) represent the value of +11 (-11) and +22 (-22), respectively.

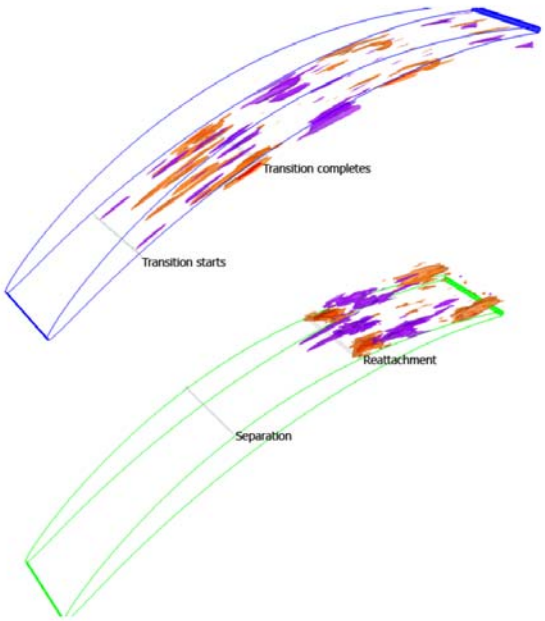


Fig.6 Isosurfaces of tangential component of the eigenmode 2. Orange (purple) and dark orange (purple) represent the value of +8.5 (-8.5) and +12 (-12), respectively.

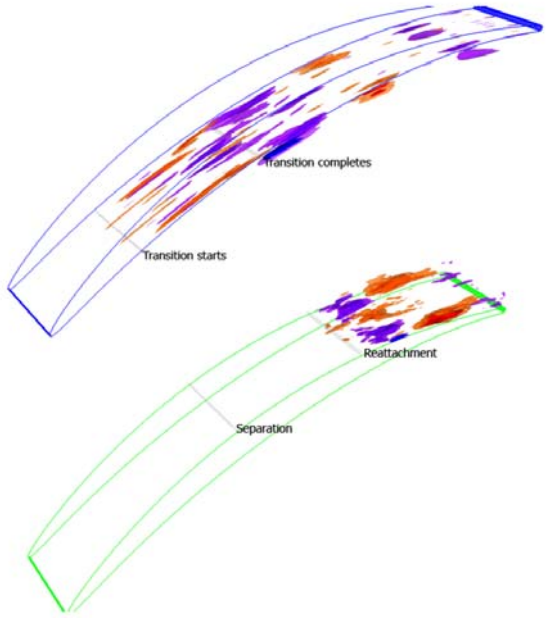


Fig.7 Isosurfaces of tangential component of the eigenmode 3 with same color levels as in Fig. 6.

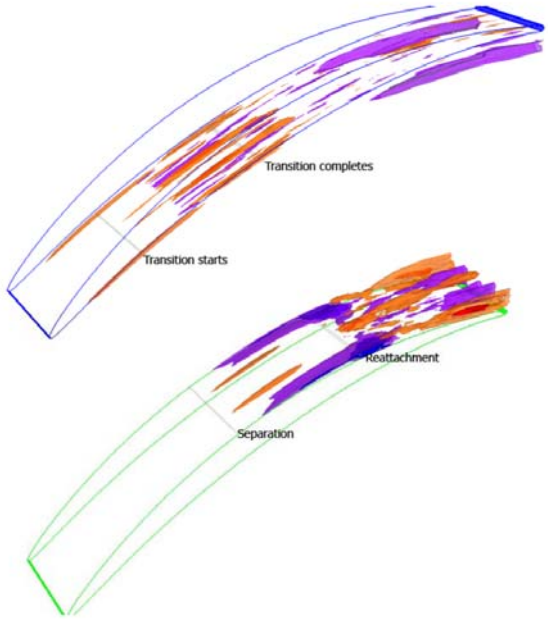


Fig.8 Isosurfaces of tangential component of the eigenmode 4 with same color levels as in Fig. 5.

**5. Conclusion and remarks**

The coherent structures of a flow through a linear compressor cascade are extracted from DNS data of [2] by means of the POD. The sparse distribution of the eigenvalues indicates that the flow is relatively complex and required many modes to accurately capture its dynamics. However the energy contents of the first three modes stand out those of the other modes hinting this study to focus on the coherent structures from the first three eigenmodes. However spectral analysis suggests the fourth mode should be as well included as it is closely associated with the first mode.

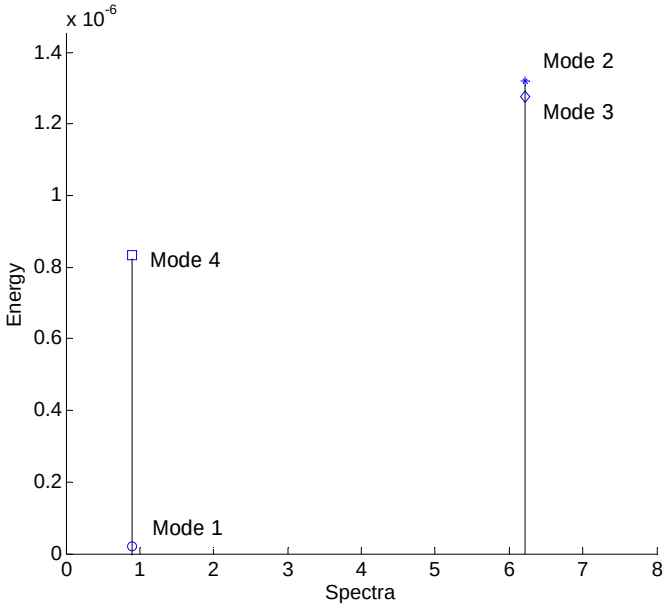


Fig.9 Energy spectrum of dominant eigenmodes.

The pressure side is undergoing a bypass transition, the coherent structures exhibit the feature of Klebanoff modes and travelling-wave structures with high activity in transition zone. On the other hand, the suction side is undergoing a separation-induced transition, the coherent structures also exhibit Klebanoff modes and travelling-wave structures. Klebanoff modes have high activity level in the separation bubble while travelling-wave structures have high activity level close to reattachment point as well as downstream of the reattachment point which may suggest high activity in breaking down into

of Kelvin-Helmholtz instability and a reattached turbulent boundary layer, respectively.

Further analysis still needs to be carried. In particular, localised POD will be performed on two sub-domains namely boundary layer of pressure and suction side sub-domains. By isolating two different transition mechanisms and their interaction in these two sub-domains, POD should perform much better allowing most energy to be contained in the first few modes. Hence the dynamics of the coherent structures and transition mechanisms can be described in a much more compact form.

## 6. Acknowledgement

Authors would like to acknowledge Dr. Tamer Zaki for making the DNS database in [2] available for this study and providing many assistance and suggestion. The authors would also like to express their gratitude to the HPC services from the Large-scale Simulation Research Laboratory of National Electronics and Computer Technology center for providing computing resources for this project.

## 7. References

[1] Mayle, R. E. (1991). The Role of Laminar-Turbulent Transition in Gas Turbine Engines, *ASME J. Turbomach*, Vol. 113, October 1991, pp. 509 – 536.

[2] Zaki, T. A., Durbin, P. A., Wissink, J. G. and Rodi, W. (2006). Direct Numerical Simulation of By-Pass and Separation-Induced Transition in a Linear Compressor Cascade, paper presented in *ASME Turbo Expo 2006: Power for Land, Sea, and Air, GT2006-99885*, Barcelona, Spain.

[3] Zaki, T. A., Wissink, J. G., Durbin, P. A. and Rodi, W. (2009). Direct Computations of Boundary Layers Distorted by Migrating Wakes in a Linear Compressor Cascade, Flow *Turbulence Combust*, Vol. 83, pp 307 – 322.

[4] Holmes, P., Lumley, J. L. and Berkooz, G. (1996). *Turbulence, Coherent Structures, Dynamical Systems and Symmetry*. Cambridge University Press, Cambridge, UK.

[5] Rempfer, D. and Fasel, H. F. (1994). Evolution of Three-Dimensional Coherent Structures in a Flat-Plate Boundary Layer, *J. Fluid Mech*, Vol. 260, pp. 351 – 375.

[6] Rempfer, D. and Fasel, H. F. (1994). Dynamics of Three-Dimensional Coherent Structures in a Flat-Plate Boundary Layer, *J. Fluid Mech*, Vol. 275, pp. 257 – 283.

[7] Hilgenfeld, L. and Pfitzner, M. (2004). Unsteady Boundary Layer Development Due to Wake Passing Effects on a Highly Loaded Linear Compressor Cascade, *ASME J. Turbomach*, Vol. 126, October 2004, pp. 493 – 500.

[8] Rosenfeld, M., Kwak, D. and Vinokur, M. (1991). A Fractional Step Solution Method for the Unsteady Incompressible Navier-Stokes Equations in Generalized Coordinate Systems, *J. Comp. Phys.*, Vol. 94, pp 102 – 137.

[9] Sirovich, L. (1987). Turbulence and the Dynamics of Coherent Structures: Part I-III, *Quaterly of Applied Mathematics*, Vol. 45(3), pp. 561 – 590.

[10] Sirovich, L., Ball, K. S. and Handler, R. A. (1991). Propagating Structures in Wall-Bounded Turbulent Flows, *Theoret. Comput. Fluid Dynamics*, Vol. 2, pp 307 – 317.